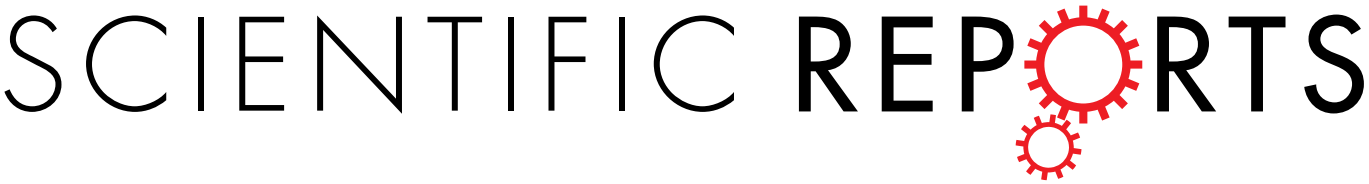

OPEN

Received: 30 April 2016
Accepted: 10 October 2016
Published: 02 November 2016

Pollutant-induced cell death and reactive oxygen species accumulation in the aerial roots of Chinese banyan (*Ficus microcarpa*)

Nan Liu[1,*], Ce Cao[1,2,*], Zhongyu Sun[3], Zhifang Lin[1] & Rufang Deng[1]

Industrial pollutants induce the production of toxic reactive oxygen species (ROS) such as $O_2^{\cdot-}$, H_2O_2, and $^{\cdot}OH$ in plants, but they have not been well quantified or localized in tissues and cells. This study evaluated the pollutant- (HSO_3^-, NH_4NO_3, Al^{3+}, Zn^{2+}, and Fe^{2+}) induced toxic effects of ROS on the aerial roots of Chinese banyan (*Ficus microcarpa*). Root cell viability was greatly reduced by treatment with 20 mM $NaHSO_3$, 20 mM NH_4NO_3, 0.2 mM $AlCl_3$, 0.2 mM $ZnSO_4$, or 0.2 mM $FeSO_4$. Biochemical assay and histochemical localization showed that $O_2^{\cdot-}$ accumulated in roots in response to pollutants, except that the staining of $O_2^{\cdot-}$ under $NaHSO_3$ treatment was not detective. Cytochemical localization further indicated that the generated $O_2^{\cdot-}$ was present mainly in the root cortex, and pith cells, especially in NH_4NO_3- and $FeSO_4$-treated roots. The pollutants also caused greatly accumulated H_2O_2 and $^{\cdot}OH$ in aerial roots, which finally resulted in lipid peroxidation as indicated by increased malondialdehyde contents. We conclude that the *F. microcarpa* aerial roots are sensitive to pollutant-induced ROS and that the histochemical localization of $O_2^{\cdot-}$ via nitrotetrazolium blue chloride staining is not effective for detecting the effects of HSO_3^- treatment because of the treatment's bleaching effect.

China is experiencing serious pollution problems caused by petrochemical smelting, mining, manufacturing, and other activities associated with rapid industrialization. In 2015, China emitted an estimated 18.59 million tons of sulfur dioxide (SO_2), and 18.51 million tons of nitrogen oxides (NO_x), and had critical levels of soil pollution by heavy metal[1]. Industrial pollutants, such as SO_2, NO_x, NH_3, and metal ions, are thought to directly or indirectly threaten the health of plants; the symptoms include damaged chloroplast ultrastructure[2], reduced cell viability[3,4], reduced water-use efficiency[5], and increased carbon construction costs[6]. Specifically, atmospheric SO_2 can easily penetrate membranes and convert into bisulfite and sulfite ions in cells[7,8]. By opening S-S bridges (sulfitolysis), sulfite can inactivate the proteins in the thioredoxin system and thereby change redox status, light-dark regulation, and chloroplast metabolism[9,10]. Atmospheric deposition of nitrogen can directly affect the plant nutrient uptake, growth, and metabolism of plants[11]. The assimilation of NH_4^+ can cause cellular acidosis, which alters acid-base regulation in plant cells[12]. Some metals such as aluminium (Al) are redox-inactive and lack metabolic function in plants. Aluminium ion (Al^{3+}) or its hydrated form $AlCl(H_2O)_6^{3+}$ in acidic tropical soil is toxic to plants causing damage to the cell wall, cytosol, and root cytoskeleton[13,14]. Unlike Al, redox-active metals like Zn and Fe are involved in plant metabolism[15]. High levels of Zn can compete with iron, leading to decreased metabolisms in plants[16]. Although plants require Fe, high levels of Fe in soil may cause deficiencies of other nutrients, including P, K, Ca, Mg, and Zn[17].

Some of the damage caused by industrial pollution to trees results from the induction of oxidative processes that reduce peroxidic bonds and that consequently catalyse the production of reactive oxygen species (ROS), such as superoxide ($O_2^{\cdot-}$), hydrogen peroxide (H_2O_2), and hydroxyl radical ($^{\cdot}OH$)[2,3,18]. SO_2 phytotoxicity is mainly attributed to the production of intracellular $O_2^{\cdot-}$, and its detoxification is primarily dependent on the oxidative conversion of SO_3^{2-} and HSO_3^- into non-harmful sulfate (SO_4^{2-})[19] Oxides of nitrogen (NO and NO_2) also cause

[1]Key Laboratory of Vegetation Restoration and Management of Degraded Ecosystems, South China Botanical Garden, Chinese Academy of Sciences, Guangzhou, 510650 China. [2]University of the Chinese Academy of Sciences, Beijing, 100049 China. [3]Guangdong Open Laboratory of Geospatial Information Technology and Application, Guangzhou Institute of Geography, Guangzhou, 510070 China. *These authors contributed equally to this work. Correspondence and requests for materials should be addressed to N.L. (email: liunan@scbg.ac.cn)

oxidative stress to plants. NO can rapidly react with $O_2^{\cdot-}$ to form $ONOO^-$, which may transform to $^{\cdot}OH$, the most reactive and toxic ROS[20,21]. Moreover, in the presence of nitrate (NO_3^-) assimilation, $^{\cdot}OH$ can be generated and cause free radical-induced injury[22]. Zn and Fe are redox-active metals, and redox cycling catalyses the production of ROS through the Fenton reaction or the peroxidase-catalysed reaction in the presence of O_2 and NADH[23]. As a redox-inactive metal, Al cannot directly participate in biological redox reactions with oxygen, but it can inhibit antioxidant enzymes, causing the accumulation of ROS in cells. ROS can cause cell death and organ senescence, because they readily participate in chain reactions between free radicals and membrane lipids and proteins, resulting in the breakdown of membranes, disturbance of mitosis, inhibition of DNA synthesis, and inactivation of enzymes[4,20,24].

The deposition of atmospheric sulfur, nitrogen, and industrial dust containing metals has caused the decline of indigenous tree species in South China, but the mechanisms are incompletely understood[5,6,25]. Our previous studies indicated that different forms of pollutants, alone or in combinations, are involved in accelerating oxidative process, causing decreased rates of electron transport and damaged membrane systems in leaf cells[2,5,6]. The toxic effects of ROS caused by various pollutants on aerial roots, however, have been rarely investigated or compared[18]. Aerial roots directly contact air and soil pollutants, and their growth was found to be restricted in industrially polluted regions in subtropical China[26]. In the current study, we evaluated the oxidative stress induced by various industrial pollutants in the aerial roots of Chinese banyan. Chinese banyan is a common landscape tree with a unique aerial root system that grows downward along the trunk to the soil[27]. We also compare methods for quantifying ROS.

Methods

Plant material and pollutants. Chinese banyan, *Ficus microcarpa* Linn. f. (Moraceae), is a native evergreen tree that is used for urban greening in South China[27]. In April 2015, newly sprouted aerial roots were removed from 15 mature trees growing in the South China Botanical Garden, Guangzhou, China. Each aerial root segment was 5 cm long had a root tip on one end. The root segments were quickly transferred to the laboratory and rinsed with distilled water and then wiped dry.

The aerial root samples (6–8 for per tree from 15 trees) were vacuum-infiltrated for 30 min with distilled water (control, pH 6.09), 20 mM $NaHSO_3$ (pH 3.08), 20 mM NH_4NO_3 (pH 4.86), 0.2 mM $AlCl_3$ (pH 4.07), 0.2 mM $ZnSO_4$ (pH 5.48), or 0.2 mM $FeSO_4$ (pH 4.47). Vacuum infiltration was used in order to decrease the differences in the penetration rates of the different ions into the root segments and shorten the treatment period. We referred the atmospheric sulfur and nitrogen, and surface soil metal concentrations in industrially polluted site in South China as background information[2,5,18,26,28]. Based on these reported and our preliminary data, we treated our aerial root samples by designated pollutant concentrations as mentioned above. During treatment, the root samples were kept in an incubator (10 h light and 14 h dark) at 25 °C. A subsample of each root sample (a 3-cm length from the root tip) was then used to determine aerial root viability, the histochemical localization of ROS, and ROS content as described in the following sections.

Aerial root viability. Aerial root viability was determined by Evans blue staining[29]. The 3-cm-long subsamples (five per treatment) were immersed in a 0.25% solution of Evans blue (E2129, Sigma); after 12 h, the subsamples were washed with distilled water to remove the Evans blue solution from the root surface. The dyed root samples were photographed with a digital camera (DSC-F717, Sony, Japan) and then chopped into small pieces and placed in a 1% sodium dodecyl sulfate (SDS) solution for 24 h to completely extract the blue stain. The blue extract, which represented dead cells, was quantified with a spectrophotometer (Lambda 650, Perkin-Elmer, USA) at 600 nm.

Histochemical and cytochemical localization of $O_2^{\cdot-}$. $O_2^{\cdot-}$ was localized by staining with nitrotetrazolium blue chloride (NBT, N6876, Sigma)[18]. The 3-cm-long subsamples (five per treatment) were immersed in HEPES-NaOH buffer (pH 7.6) containing 0.5 mg of NBT/ml and 10 mM NaN_3. The subsamples were vacuum infiltrated in this NBT solution for 30 min and were then held at room temperature until the blue colour (NBT-$O_2^{\cdot-}$) became visible. The NBT-stained roots were photographed with a digital camera (DSC-F717, Sony, Japan) before semi-thin transverse sections (8 μm thick) were prepared. Semi-thin section was conducted by fixing aerial root samples in 0.1 M phosphate buffer (pH 7.2) containing 2% glutaraldehyde and 2.5% Paraformaldehyde. After 6 times wash with 0.1 M phosphate buffer, they were dehydrated by alcohol steeply and eddied in flat molds using EPON812 resin. Sctions (2 μm) were cut by ultramicrotome (Leica, UC6, Germany). The sections were observed and photographed with a light microscope (AX70, Olympus, Japan) and a digital camera (DP50, Olympus, Japan).

Histochemical localization of H_2O_2. H_2O_2 was localized by staining with 3,3′,5,5′-Tetramerthyl benzidine dihydrochloride hydrate (TMB, V900355, Sigma)[30]. The 3-cm-long subsamples (five per treatment) were immersed in 10 mM sodium-citrate buffer (pH 4.0) containing 1 mM TMB at room temperature until the TMB-H_2O_2 formazan became visible. The stained roots were then photographed with a digital camera (DSC-F717, Sony, Japan).

$^{\cdot}OH$ and H_2O_2 quantification. $^{\cdot}OH$ was quantified using terephthalic acid (TPA) as a hydroxyl radical dosimeter as described in previous studies[21,29]. The 3-cm-long subsamples (five per treatment) were homogenized in phosphate buffer (50 mM, pH 7.0), and the supernatant was collected after centrifugation at 10000 *g* for 10 min at 4 °C. The 0.2-ml extracts were incubated in a 2-ml solution containing 0.2 ml of 50 μM TPA and 1.6 ml of phosphate buffer (50 mM, pH 7.0). After incubation for 10 min, the fluorescence emission spectra from 350 to 550 nm of monohydroxy terephthalate (TPA-$^{\cdot}OH$) was recorded with a fluorescence spectrophotometer (LS 55, Perkin-Elmer, USA) with an excitation wavelength of 326 nm.

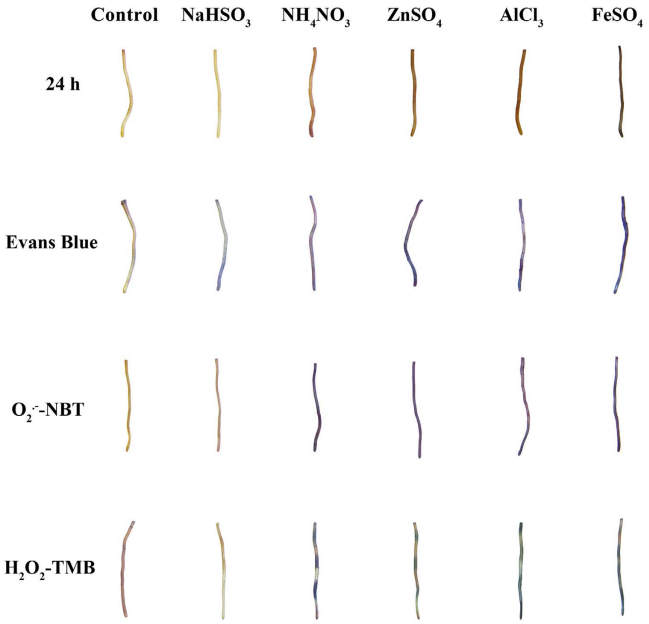

Figure 1. Surface colour (first row), cell viability (second row), and histochemical localization of $O_2^{\cdot-}$ (third row) and H_2O_2 (last row) in aerial roots of *F. microcarpa* treated with purified water (Control), 20 mM $NaHSO_3$, 20 mM NH_4NO_3, 0.2 mM $ZnSO_4$, 0.2 mM $AlCl_3$, or 0.2 mM $FeSO_4$. The roots were photographed after 24 h of treatment. Cell viability is indicated by the Evans blue staining. $O_2^{\cdot-}$ and H_2O_2 accumulations are indicated by the formation of NBT-$O_2^{\cdot-}$ and TMB-H_2O_2.

H_2O_2 was detected using a fluorescence spectrophotometer (LS 55, Perkin-Elmer, USA) as previously described[18,31]. The 3-cm-long subsamples (five per treatment) were homogenized in phosphate buffer (20 mM, pH 6.0). After the homogenate was centrifuged at 10000 *g* for 10 min at 4 °C, 5 ml of the supernatant was collected. The 3-ml reaction mixture also included 0.2 ml of root extract, 5 μM scopoletin (S2500, Sigma), and 3 μg ml^{-1} horseradish peroxidase. The fluorescence emission spectra were recorded from 400 to 550 nm with an excitation wavelength of 346 nm.

Detection of $O_2^{\cdot-}$ accumulation. Root sample extracts were obtained after homogenization in phosphate buffer (20 mM, pH 6.0). The 0.2-ml extracts were then incubated for 5 h in the dark in 2 ml of phosphate buffer (20 mM, pH 6.0) containing 0.5 mM Na, 39- [1-[(phenylamino)-carbonyl]-3,4-tetrazolium]-bis (4-methoxy-6-nitro) benzenesulfonic acid hydrate (XTT, X4626, Sigma). Formation of XTT-$O_2^{\cdot-}$-formazan was detected using a UV spectrophotometer (Lambda 650, Perkin-Elmer, USA) at 470 nm[18,31].

Malondialdehyde (MDA) quantification. Root samples were homogenized with 0.5% (w/v) thiobarbituric acid in 20% (w/v) trichloroacetic acid. The mixture was incubated at boiling water for 30 min and then quickly cooled in a refrigerator. After centrifugation at 1800 g for 10 min, the supernatant was used for MDA determination using a UV spectrophotometer (Lambda 650, Perkin-Elmer, USA)[32].

Data analysis. Results are shown as means ± standard deviations (SDs). One-way analyses of variance (ANOVAs) were used to determine the effects of treatment on Evans blue staining, XTT-$O_2^{\cdot-}$ formation and MDA quantification. When effects were significant, means were compared with the Tukey's test. All statistical analyses were performed by SPSS 19.0 (SPSS, Inc., USA). Differences were considered significant at $P < 0.05$.

Results

Aerial root viability. The surface colour of roots incubated in NH_4NO_3, $ZnSO_4$, $AlCl_3$, or $FeSO_4$ became darker relative to the control, while the surface colour of roots incubated in $NaHSO_3$ became lighter (Fig. 1). As indicated by Evans blue staining, the pollutants reduced cell viability (Fig. 1). The blue staining mainly occurred in the root tips after treatment with $NaHSO_3$ but occurred throughout the 3-cm-long subsample following treatment with NH_4NO_3, $ZnSO_4$, $AlCl_3$, or $FeSO_4$. The absorbance of the blue extract (600 nm) confirmed that all of the pollutants significantly reduced the viability of the aerial roots ($P < 0.05$, Fig. 2A). Moreover, the viability was lower following $NaHSO_3$, $ZnSO_4$, and $FeSO_4$ treatment than following NH_4NO_3 or $AlCl_3$ treatment.

Histochemical and cytochemical localization of $O_2^{\cdot-}$. When dyed with NBT, root segments treated with NH_4NO_3, $ZnSO_4$, $AlCl_3$, or $FeSO_4$ but not with $NaHSO_3$ became blue, indicating the presence of $O_2^{\cdot-}$ (Fig. 1). The blue was most intense in roots treated with NH_4NO_3 and $FeSO_4$. Semi-thin transverse sections indicated that large quantities of blue formazan (NBT-$O_2^{\cdot-}$) accumulated in the root tips following treatment with NH_4NO_3 (Fig. 3G–I) and the metal pollutants (Fig. 3J–R) and that most of the $O_2^{\cdot-}$ was in the root cortex and pith cells. In contrast, cross sections of control root tips or those treated with $NaHSO_3$ were not blue (Fig. 3A–F). In agreement

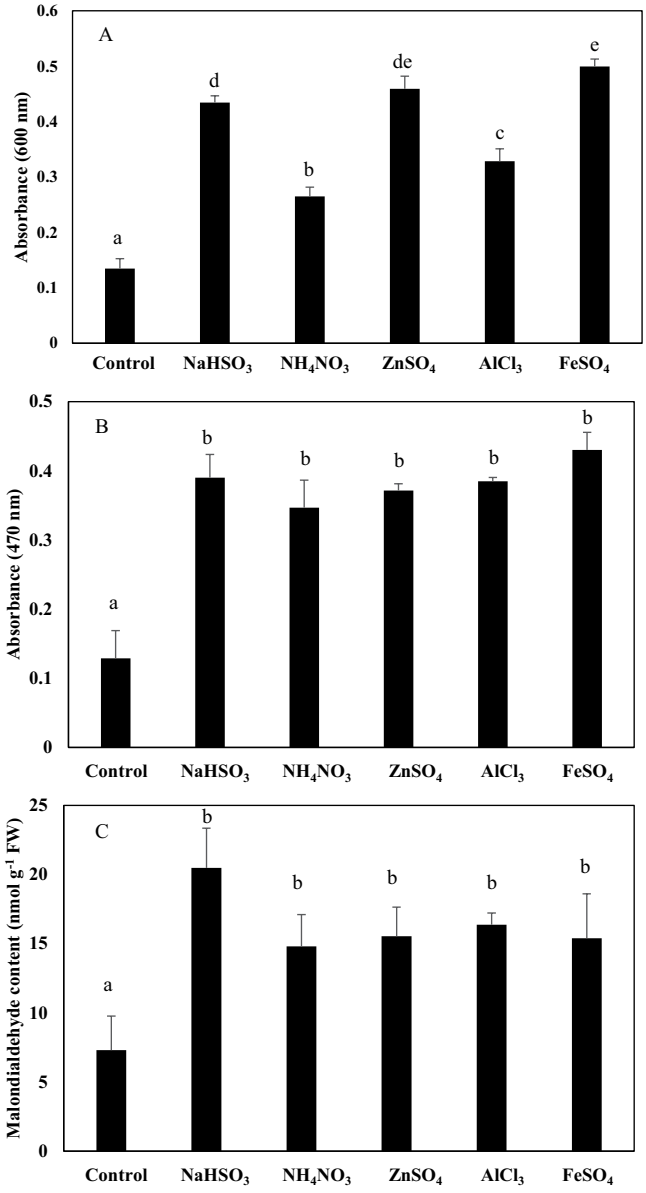

Figure 2. Cell viability indicated by absorbance of the Evans blue extract at 600 nm (**A**), $O_2^{\cdot-}$ accumulation as indicated by absorbance of XTT-$O_2^{\cdot-}$-formazan at 470 nm (**B**), and levels of lipid peroxidation as indicated by malondialdehyde content (**C**) in aerial roots of *F. microcarpa* treated with purified water (Control), 20 mM $NaHSO_3$, 20 mM NH_4NO_3, 0.2 mM $ZnSO_4$, 0.2 mM $AlCl_3$, or 0.2 mM $FeSO_4$. Values are means + SD; n = 6. Means with different letters are significantly different at $P < 0.05$.

with the histochemical observations, the cytochemical localizations of $O_2^{\cdot-}$ indicated that accumulation of $O_2^{\cdot-}$ was greater following treatment with NH_4NO_3 and $FeSO_4$ than in the control. Although large quantities of ROS were generated in the root tips following treatment with the pollutants for 24 h, pollutant-induced damage to cell structure was not evident in the enlarged microscopic pictures (Fig. 3C,I,L,O,R).

Histochemical localization and quantification of $O_2^{\cdot-}$ and $^{\cdot}OH$. As indicated by XTT-$O_2^{\cdot-}$-formazan absorbance at 470 nm, $O_2^{\cdot-}$ accumulation in aerial root cells was significantly higher in all of the pollutant treatments than in the control ($P < 0.05$, Fig. 2B). The significantly elevated $O_2^{\cdot-}$ accumulation induced by the pollutants is consistent with the NBT staining of root cross sections (Fig. 1).

To assess the accumulation of $^{\cdot}OH$, fluorescence spectra were detected by adding TPA to the root extracts. The TPA-$^{\cdot}OH$ fluorescent emission curves peaked at 463 nm, and the intensities were much higher for roots treated with pollutants than for control roots (Fig. 4A). The peak of the relative fluorescent values of TPA-$^{\cdot}OH$ was higher for $FeSO_4$ than for the other pollutants.

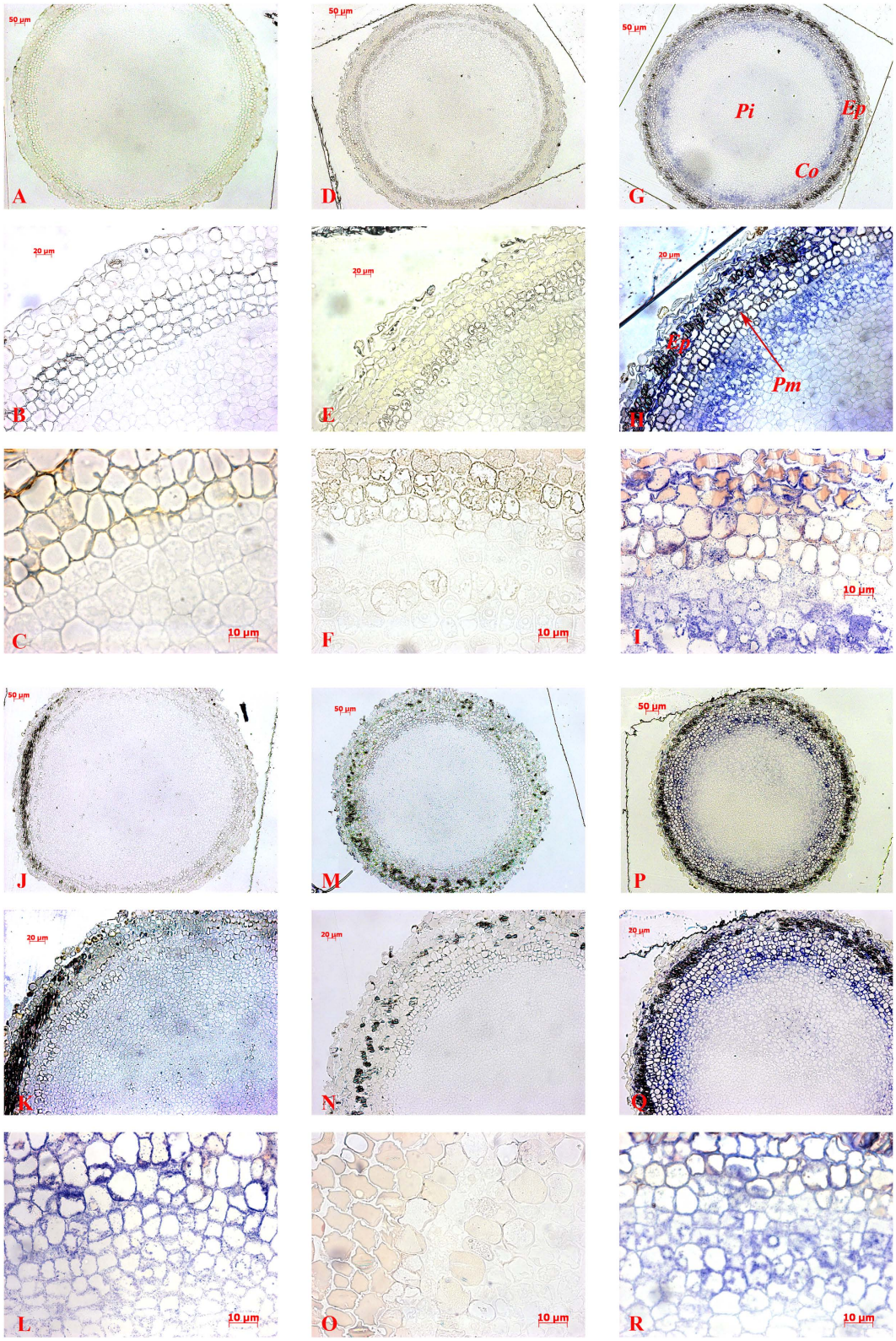

Figure 3. Cytochemical localization of $O_2^{\cdot-}$ in aerial root cells (cross section behind root tips) of *F. microcarpa* treated with purified water (**A–C**), 20 mM $NaHSO_3$ (**D–F**), 20 mM NH_4NO_3 (**G–I**), 0.2 mM $ZnSO_4$ (**J–L**), 0.2 mM $AlCl_3$ (**M–O**), or 0.2 mM $FeSO_4$ (**P–R**). (**C,F,I,L,O,R**) are enlarged pictures of corresponding (**B,E,H,K,N,Q**) by the order of 100 times, respectively. Co: cortex; Ep: epidermis; Pi: pith; Pm: plasma membrane.

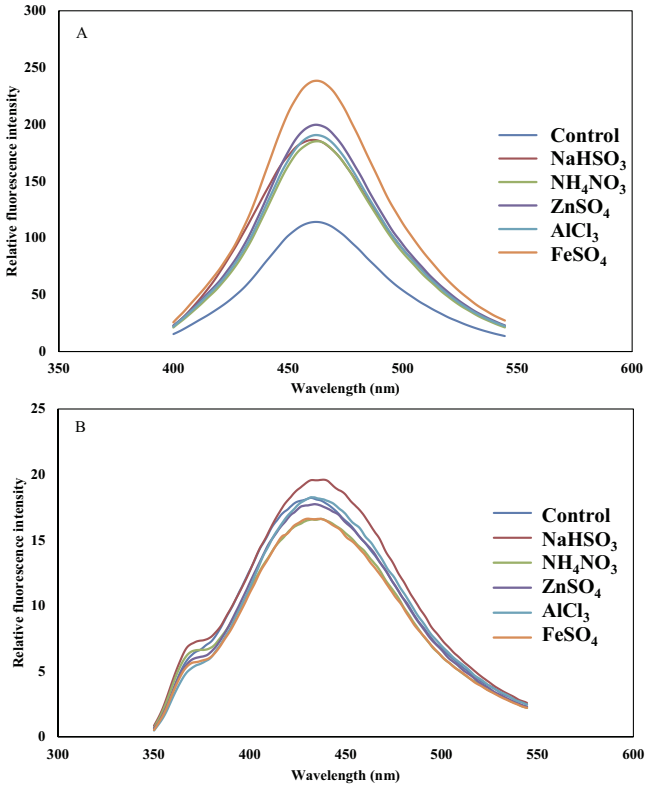

Figure 4. ·OH accumulation as indicated by the fluorescence intensity of TPA-·OH formazan at 463 nm (**A**), and H_2O_2 accumulation as indicated by the fluorescence intensity of H_2O_2-scopoletin formazan at 433 nm (**B**) in aerial roots of *F. microcarpa* treated with purified water (Control), 20 mM $NaHSO_3$, 20 mM NH_4NO_3, 0.2 mM $ZnSO_4$, 0.2 mM $AlCl_3$, or 0.2 mM $FeSO_4$. Each curve is the average of 5–6 replicates.

Quantification of H_2O_2. The accumulation of H_2O_2 was assessed using fluorescence spectra by adding scopoletin to the root extracts. H_2O_2 accumulation (based on relative fluorescence intensity at 433 nm) in aerial root segments did not substantially differ between the control and the other treatments (Fig. 4B). Different from fluorescent assays, the histochemical staining of TMB-H_2O_2 showed that root segments treated with NH_4NO_3, $ZnSO_4$, $AlCl_3$, or $FeSO_4$ was obvious, indicating the presence of H_2O_2. By contrary, the staining of TMB-H_2O_2 on $NaHSO_3$ treated root samples was not detected (Fig. 1).

Quantification of MDA. The MDA contents of pollutant-treated aerial root samples were mostly higher than that of controls. The significantly increased MDA levels were detected in all pollutant treated root samples, indicating higher oxidative damage and lipid peroxidation (Fig. 2C).

Discussion

In this study, aerial roots of Chinese Banyan obviously suffered from treatment with pollutants as indicated by darker root surfaces (except in the case of $NaHSO_3$), dehydration symptoms (especially in the case of $FeSO_4$), and accumulation of ROS. Bisulfite (HSO_3^-) is the byproduct of SO_2 in cells, and the derivative is directly and indirectly toxic to plant tissues[2]. SO_2 and its derivate HSO_3^- harm leaves by generating excessive quantities of ROS, resulting in the bleaching of photosynthetic pigments[33,34]. Our study found, for the first time to our knowledge, that aerial root systems were also harmed by bleaching caused by HSO_3^-, the cell death caused by $NaHSO_3$ was confirmed by Evans blue staining (Fig. 1). Similarly, Evans blue staining in this study indicated that the viability of aerial root cells was decreased by NH_4NO_3, $ZnSO_4$, $AlCl_3$, and $FeSO_4$ (Fig. 1). The decrease of aerial root cell viability was mainly caused by the decrease of cell pH, imbalance of mineral assimilation, as well as injuries in cell wall, plasma membrane, and signal transduction pathways[11–16].

Under biotic and abiotic stress, plant cells produce ROS in several subcellular compartments[35]. As revealed by previous studies, redox-active metals (e.g., Fe^{2+} and Zn^{2+}) as well as redox-inactive metals (e.g., Al^{3+}) may induce the activity of plasma membrane-localized NADPH oxidase, which transfers electrons from cytosolic NADPH to O_2 and subsequently forms $O_2^{\cdot-}$[36,37]. In our study, the deep-blue staining of NBT-$O_2^{\cdot-}$-formazan in the aerial roots that were treated with metal pollutants was documented by histochemical staining and by cytochemical observation of micrographs; our cytochemical observations were consistent with previous reports that NBT-$O_2^{\cdot-}$ is mainly found in cells[18]. Thus, we infer that the increased absorbance by XTT-$O_2^{\cdot-}$ at 470 nm and the formation of NBT-$O_2^{\cdot-}$ can be attributed to the activation of NADPH oxidase by metal ions in aerial roots. High concentrations of $NaHSO_3$ and NH_4^+ have been reported to damage cells because HSO_3^- detoxification and NO_3^- assimilation cause the generation of free radicals[2,12,20]. In accordance with these studies, our results showed

that all pollutants caused massive accumulations of $O_2^{\cdot-}$ in cells, as indicated by biochemical assay (Fig. 2B) and by histochemical staining (Fig. 3). The exception was that only low levels of $O_2^{\cdot-}$ were detected in $NaHSO_3$ treated root segments: even though XTT-$O_2^{\cdot-}$ absorbance was high, NBT-$O_2^{\cdot-}$-formazan was almost undetectable by histochemical and cytochemical observation (Fig. 3D–F). $NaHSO_3$ is usually used as an additive bleaching agent. Therefore, we suspect that the bleaching caused by HSO_3^- may result in the failure of NBT staining and that NBT-$O_2^{\cdot-}$ staining is not suitable for $O_2^{\cdot-}$ detection in SO_2- or HSO_3^--treated tissues.

In our study, H_2O_2 accumulation was not detected in pollutant-treated tissues by the fluorometric scopoletin oxidation assay (Fig. 4B). The histochemical staining, however, clearly indicated the production of H_2O_2 in pollutant-treated aerial root samples. Here, we infer that H_2O_2 detective method by fluorescence intensity of H_2O_2-formazan may not always be effective, because the peroxide activity might be enhanced during the preparation of root extract, causing more consumption of H_2O_2 and reduced fluorescence intensity of H_2O_2-fomazan. This result was also in agree with previous study that H_2O_2 is a versatile member of ROS network and that H_2O_2 increased in plant tissues under Al stress[38–40].

$^{\cdot}OH$ is among the most toxic of the ROS because of its capacity to initiate radical chain reactions that result in irreversible chemical modifications of various cellular components[41]. Because different pollutants (SO_2, NH_4NO_3, and metal ions) are all involved in the accumulation of ROS within plant cells[2,20,29], the induced oxidative processes finally break the free radical chains of membrane lipids, causing membrane decomposition (increased MDA content, Fig. 2C) and cell death (decreased cell viability, Fig. 2A). In our study, TPA-$^{\cdot}OH$ fluorescence was greatly increased by all five pollutants, indicating that these pollutants increased $^{\cdot}OH$ accumulation in aerial root tissues (Fig. 4A). Because Fe^{2+} is involved in the Fenton reaction, $FeSO_4$ treatment greatly increased $^{\cdot}OH$ concentrations in aerial root tissues. NH_4NO_3 treatment also greatly increased $^{\cdot}OH$ accumulation in aerial root tissue, which is consistent with previous findings that nitrate assimilation directly interferes with free radical metabolism and causes free radical-induced injury[20].

Overall, the pollutant treatments in the current study caused ROS accumulation and profound oxidative damage, and finally cell death in aerial root tissues. Because $O_2^{\cdot-}$ is the initial ROS generated during O_2 metabolism in plant tissue, quantification of $O_2^{\cdot-}$ is vital for assessing ROS damage in plant tissues subjected to various stresses. In our study, we used both XTT and NBT to detect the accumulation of $O_2^{\cdot-}$. XTT is more sensitive than NBT, and XTT-$O_2^{\cdot-}$ can be quantitatively detected using spectrochemical methods. NBT staining may be suitable for the qualitative assessment of $O_2^{\cdot-}$ accumulation in plant tissues that have been subjected to most stresses but not to $NaHSO_3$. The bleaching effect of HSO_3^- reduced the effectiveness of NBT staining in plant tissues. This study also showed that the aerial roots of *Ficus microcarpa* are sensitive to various pollutants and that aerial roots may be good indicators of pollutants in industrially polluted regions.

References

1. Ministry of Environmental Protection of People's Republic of China. *2015 Report on the state of the environment of China* (2016).
2. Liu, N., Lin, Z. F., Guan, L. L., Lin, G. Z. & Peng, C. L. Light acclimation and HSO_3^- damage on photosynthesis apparatus of three subtropical forest species. *Ecotoxicology* **18,** 929–938 (2009).
3. Schützendübel, A. & Polle, A. Plant responses to abiotic stresses: heavy metal induced oxidative stress and protection by mycorrhization. *J Exp Bot* **53,** 1351–1365 (2002).
4. Islam, E. *et al.* Effect of Pb toxicity on leaf growth, physiology and ultrastructure. *J Hazard Mater* **154,** 914–926 (2008).
5. Sun, F. F. *et al.* Long-term tree growth rate, water use efficiency, and tree ring nitrogen isotope composition of *Pinus massoniana* L. in response to global climate change and local nitrogen deposition in Southern China. *J Soils Sediments* **10,** 1453–1465 (2010).
6. Liu, N., Guan, L. L., Sun, F. F. & Wen, D. Z. Alterations of chemical composition, construction cost and payback time in needles of Masson pine (*Pinus massoniana* L.) trees grown under pollution. *J Plant Res* **127,** 491–501 (2014).
7. Hamisch, D. *et al.* Impact of SO_2 on *Arabidopsis thaliana* transcriptome in wild type and sulfite oxidase knockout plants analyzed by RNA deep sequencing. *New Phytol* **196,** 1074–1085 (2012).
8. Randewig, D. *et al.* Sulfite oxidase controls sulfur metabolism under SO2 exposure in *Arabidopsis thaliana*. *Plant Cell Environ* **35,** 100–115 (2012).
9. Malhotra, S. S. & Khan, A. A. Biochemical and physiological impacts of major pollutants. In *Air pollution and plant life* (ed. Treshow, M.) 113–157 (1984).
10. Würfel, M., Haberlein, I. & Follmann, H. Inactivation of thioredoxin by sulfite ions. *FEBS Letters* **268,** 146–148 (1990).
11. Sardans, J. & Peñuelas, J. The role of plants in the effects of global change on nutrient availability and stoichiometry in the plant-soil system. *Plant Physiol*, **160,** 1741–1761 (2012).
12. Pearson, J. & Stewart, G. R. The deposition of atmospheric ammonia and its effects on plants. *New Phytol* **125,** 283–305 (1993).
13. Matsumoto, H. & Motoda, H. Oxidative stress is associated with aluminum toxicity recovery in apex of pea root. *Plant Soil* **363,** 399–410 (2013).
14. Kochian, L. V., Piñeros, M. A. & Hoekenga, O. A. The physiology, genetics and molecular biology of plant aluminum resistance and toxicity. *Plant Soil* **274,** 175–195 (2005).
15. Påhlsson, A. M. B. Toxicity of heavy metals (Zn, Cu, Cd, Pb) to vascular plants. *Water Air Soil Pollut* **47,** 287–319 (1989).
16. Stiborova, M., Doubravova, M. & Leblova, S. A comparative study of the effect of heavy metal ions on ribulose-1,5-bisphosphate carboxylase and phosphoenol pyruvate carboxylase. *Biochem Physiol Pflanz* **181,** 373–379 (1986).
17. Sahrawat, K. L. *et al.* The role of tolerant genotypes and plant nutrients in the management of iron toxicity in lowland rice. *J Agric Sci* **126,** 143–149 (1996).
18. Liu, N., Lin, Z. F. & Mo, H. Metal (Pb, Cd, and Cu) – induced reactive oxygen species accumulations in aerial root cells of the Chinese banyan (*Ficus microcarpa*) *Ecotoxicology* **21,** 2004–2011 (2012).
19. Bharali, B. & Bates, J. W. Detoxification of dissolved SO_2 (bisulfite) by terricolous mosses. *Ann Bot* **97,** 257–263 (2006).
20. Wellburn, A. R. Why are atmospheric oxides of nitrogen usually phytotoxic and not alternative fertilizers? *New Phytol* **115,** 395–429 (1990).
21. Yang, X. F. & Guo, X. Q. Fe(II)-EDTA chelate-induced aromatic hydroxylation of terephthalate as a new method for the evaluation of hydroxyl radical—scavenging ability. *Analyst* **126,** 928–932 (2001).
22. Raven, J. A. Acquisition of nitrogen by the shoots of land plants: its occurrence and implications for acid-base regulation. *New Phytol* **109,** 1–20 (1988).
23. Schopfer, P. & Liszkay, A. Plasma membrane-generated reactive oxygen intermediates and their role in cell growth of plants. *BioFactors* **28,** 73–81 (2006).

24. Blomster, T. *et al.* Apoplastic reactive oxygen species transiently decrease auxin signaling and cause stress-induced morphogenic response in Arabidopsis. *Plant Physiol* **157,** 1866–1883 (2011).
25. Guan, L. L. & Wen, D. Z. More nitrogen partition in structural proteins and decreased photosynthetic nitrogen-use efficiency of *Pinus massoniana* under *in situ* polluted stress. *J Plant Res* **124,** 663–673 (2011).
26. Kong, G. H. *et al.* Injury symptoms of 38 woody species exposed to air pollutants. *J Trop Subtrop Bot* **11,** 319–328 (2003).
27. Ren, H., Cai, X. A., Li, C. H. & Ye, Y. S. *Atlas on tool species of vegetation recovery in South China* (Wuhan, 2010).
28. Wang, F. M. *et al.* Nitrogen and phosphorus addition impact soil N_2O emission in a secondary tropical forest of South China. *Sci Rep* **4,** 5615 (2014).
29. Liu, N. *et al.* Lead and cadmium induced alterations of cellular functions in leaves of *Alocasia macrorrhiza* L. Schott. *Ecotoxicol Environ Safe* **73,** 1238–1245 (2010).
30. Liszkay, A., Van, d. Z. E. & Schopfer, P. Production of reactive oxygen intermediates $O_2^{\cdot-}$, H_2O_2, and $^{\cdot}OH$ by maize roots and their role in wall loosening and elongation growth. *Plant Physiology* **136,** 3114–3123 (2004).
31. Schopfer, P., Plachy, C. & Frahry, G. Release of reactive oxygen intermediates (superoxide radicals, hydrogen peroxide, and hydroxyl radicals) and peroxidase in germinating radish seeds controlled by light, gibberellin, and abscisic acid. *Plant Physiol* **125,** 1591–1602 (2001).
32. Lin, Z. F., Li, S. S. & Lin, G. Z. Superoxide dismutase activity and lipid peroxidation in relation to senescence of rice leaves. *Acta Botanica Sinica* **26,** 605–615 (1984).
33. Ranieri, A. *et al.* SO_2-induced decrease in photosynthetic activity in two barley cultivars. Evidence against specific damage at the protein-pigment complex level. *Plant Physiol Biochem* **37,** 919–929 (1999).
34. Lin, Z. F. *et al.* Bisulfite (HSO_3^-) hydroponics induced oxidative stress and its effect on nutrient element compositions in rice seedlings. *Bot Stud* **52,** 173–182 (2011).
35. Murphy, T. M., Vu, H. & Nguyen, T. The superoxide synthases of rose cells. *Plant Physiol* **117,** 1301–1305 (1998).
36. Olmos, E., Martínez-Solano, J. R., Piqueras, A. & Hellín, E. Early steps in the oxidative burst induced by cadmium in cultured tobacco cells (BY-2 line). *J Exp Bot* **54,** 291–301 (2003).
37. Lin, Z. F., Liu, N., Lin, G. Z. & Peng, C. L. *In situ* localization of superoxide generated in leaves of *Alocasia macrorrhiza* (L.) Schott under various stresses. *J Plant Biol* **52,** 340–347 (2009).
38. Ma, B., Wan, J. & Shen, Z. H_2O_2 production and antioxidant responses in seeds and early seedlings of two different rice varieties exposed to aluminum. *Plant Growth Regul* **52,** 91–100 (2007).
39. Dipierro, N., Mondelli, D., Paciolla, C., Brunetti, G. & Dipierro, S. Changes in the ascorbate system in the response of pumpkin (*Cucurbita pepo* L.) roots to aluminium stress. *J Plant Physiol* **162,** 529–536 (2005).
40. Matsumoto, H. & Motoda, H. Aluminum toxicity recovery processes in root apices. Possible association with oxidative stress. *Plant Sci* **185,** 1–8 (2012).
41. Mithöfer, A., Schulze, B. & Boland, W. Biotic and heavy metal stress response in plants: evidence for common signals. *FEBS Letters* **566,** 1–5 (2004).

Acknowledgements

This study is supported by National Natural Science Foundation of China (31570585), Youth Innovation Promotion Association of the Chinese Academy of Sciences (2016311), and Guangdong Science and Technology Planning Project (2015A030303014; 2014A030305014). We are grateful to Bruce Jaffee for language editing.

Author Contributions

N.L., C.C. and Z.S., analysed data and wrote the paper. Z.L. and N.L. designed the study, proposed the scientific hypothesis and supervised the project. N.L., C.C. and R.D. carried out the experiments. N.L. and C.C. collected and determined samples. N.L., Z.S., Z.L. and R.D contributed to the interpretation of the work. All authors discussed the results and reviewed the manuscript.

Additional Information

Competing financial interests: The authors declare no competing financial interests.

How to cite this article: Liu, N. *et al.* Pollutant-induced cell death and reactive oxygen species accumulation in the aerial roots of Chinese banyan (*Ficus microcarpa*). *Sci. Rep.* **6**, 36276; doi: 10.1038/srep36276 (2016).

Publisher's note: Springer Nature remains neutral with regard to jurisdictional claims in published maps and institutional affiliations.